

The 9 September 2010 torrential rain and flash flood in the Dragone catchment, Atrani, Amalfi Coast (Southern Italy)

C. Violante¹, G. Braca², E. Esposito¹ and G. Tranfaglia²

[1]{Istituto per l'Ambiente Marino Costiero (IAMC), Consiglio Nazionale delle Ricerche (CNR), Napoli, Italy }

[2]{Istituto Superiore per la Protezione e la Ricerca Ambientale (ISPRA), Roma, Italy }

Correspondence to: C. Violante (crescenzo.violante@cnr.it)

Abstract

In this paper we use a multi-hazard approach to analyse the 9 September 2010 flash-flood ~~occurred~~ in the Dragone basin, a 9 km² catchment located along the Amalfi rocky coastal range, Southern Italy. In this area, alluvial-fan-flooding is the most frequent and destructive geologic hazards since Roman time. Sudden torrent of waters (flash flood) are caused by high-intensity and very localized cloudbursts of short duration inducing slope erosion and sediment delivery from slope-to-stream. The elevated bed load transport produces fast-moving hyperconcentrated flows with significant catastrophic implications for communities living at stream mouth.

The 9 September 2010 rainstorm event lasted 1 hours with an intensity rainfall peak nearly to 120 mm h⁻¹. High topographic relief of the Amalfi coastal range and positive anomalies of the coastal waters conditioned the character of the convective system. Based on geological data and post-event field evidence and surveys, as well as homemade-videos, and eyewitness accounts, the ~~consequent~~ flash-flood mobilized some 25.000 m³ of materials with a total (water and sediment) peak flow of 80 m³ s⁻¹. The estimated peak discharge of only clear water was about 65 m³ s⁻¹. This leads to a sediment bulking factor of 1.2 that corresponds to a flow with velocities similar to those of water during a flood.


1 Introduction

The Amalfi Coast consists of a steep mountain front (up to 1444 m a.s.l.) that rises abruptly from the Tyrrhenian Sea (Fig. 1). It is a rocky coast mostly formed by a pile of Mesozoic carbonate rocks, covered by Tertiary to Quaternary siliciclastic and pyroclastic units

1 tectonically uplifted since lower Pleistocene. Bedrock rivers and channels deeply dissect the
2 carbonate bedrock forming a complex fluvial system characterized by small catchments that
3 are very high relative to the base sea level. These rivers show a distinct seasonality and
4 torrential behaviour, with main delivery areas into the adjacent marine shelf (Fig. 2; Esposito
5 et al., 2004a,b; Budillon et al., 2005; Violante, 2009; Violante et al., 2009).

6 During the last millennia this area has been repeatedly mantled by the pyroclastic products of
7 the Somma-Vesuvius, that create favourable conditions for volcanoclastic debris to generate
8 mass flows and flash floods ~~in concomitance with rainy periods~~. The Plinian eruption that
9 destroyed the Roman cities of Pompeii, Stabiae and Herculaneum in AD 79, deposited up to 2
10 m of erosion-prone volcanoclastic material (Sigurdsson et al., 1985) on the steep coastal
11 slopes causing conditions of increased geomorphic instability.

12 Geologic evidences for rapid slope erosion following the Pompeii pyroclastic fall include
13 alluvial reworked volcanoclastic sequences (locally called Durece) occurring as residual
14 outcrops along narrow stream valleys (Cinque & Robustelli, 2009) and coastal fan-deltas fed
15 by small alluvial fans at mouth of the main streams (Sacchi et al. 2009; Violante et al., 2009).
16 These latter are composed of wedge-shaped coarse-grained alluvial deposits that thicken
17 towards the sea and represent the subaqueous counterpart of small fans at river mouths (Fig.
18 2, inset).

19 Pyroclastic air-fall tephra derived from late Quaternary activity of the Somma-Vesuvius still
20 occur as unstable sedimentary covers on top of the steep carbonate slopes of the Amalfi coast.
21 These deposits creates conditions of elevated slope instability in conjunction with rainstorm
22 events that frequently hit the Amalfi Coast ~~through historical times~~. The slides are mostly
23 shallow and very wide, extending all the way to the mountain ridge and crest, and largely
24 ascribing to soil slip, debris/earth flow phenomena. Besides rapid sediment transport along
25 valley flanks, landslide debris flowing from slope to streams produce fast-moving large debris
26 torrents (flash flood) with significant catastrophic implications for local communities mostly
27 living on alluvial deltas at stream mouths. Here flood-prone streams have been artificially
28 forced to flow underneath roads and squares to exploit the whole delta surfaces for urban
29 development (Fig. 2). 

30 In this paper we analyse the 9 September 2010 rainfall event that hit the Costa d'Amalfi and
31 its consequences in the Dragone catchment and Atrani village. Direct field observations that
32 include geological investigations and damage to property and infrastructures have been

1 combined with meteorological and hydraulic/hydrological analyses. Reconstruction and
2 recurrence of past events based on different historical sources, and marine geophysical and
3 geological data of the Dragone submerged delta have been also taken into account.

4 **2 The Dragone catchment-fan-delta system**

5 The Dragone catchment drains an area of 9.3 km² along the steep coastal slopes of the Amalfi
6 Coast. The basin develops in a North-South direction and is strongly asymmetric, with the
7 eastern flank composed of a short and abrupt slope corresponding to a fault scarp and the
8 western flank formed by four main sub-basins: ~~the~~ Scalandrone, ~~the~~ Nocelle, ~~the~~ Senite, and
9 ~~the~~ S. Caterina. A fifth sub-basin, ~~the~~ Frezzi, develops at the head of the Dragone stream
10 (Fig. 3A). The drainage area rises up to 1420 m a.s.l. and cuts into Mesozoic limestone
11 discontinuously mantled by Quaternary volcanoclastic and alluvial deposits. A low drainage
12 frequency (5 km⁻²) and a sub-dendritic pattern characterize the hydrographic network with the
13 main stream, the Dragone, discharging directly into the Tyrrhenian Sea. Slope analysis based
14 on a 5x5m cell size DTM (Digital Elevation Model) indicates that topographic gradient of the
15 catchment area is arranged into two main slope classes ranging from 15° to 35° and from 35°
16 to 50° (golden/yellow and brown colours respectively in Fig. 3B). The mean slope is 30°.

17 The Dragone stream is 6.8 km in length with the terminal section covered by a roadway
18 crossing the Atrani village. The entombment of the water course has an input section of 3 x 9
19 m (*h* x *w*) that reduces to 1.80 x 5.50 m at closing section, and a total length of about 300 m.
20 Runoff waters are regulated by concrete levees and bridges that extend over two third of the
21 hydrographic network.

22 At sea a submerged fan-delta occurs at closing section of the Dragone catchment (Sacchi et
23 al., 2009; Violante et al., 2009). The delta body is 0.2 km² wide and reach a max thickness of
24 25 m. It displays a generally conical morphology with a delta front slope of 30° and foreset
25 inclination ranging from 15° to 30°. This structure is composed of alluvial sequences that
26 coincide with significant changes in river activity during streamflow phenomena. Increases in
27 fluvial sedimentary discharge are recorded as successive phases of delta growths to which
28 associate temporary shoreline progradations.

29 Detailed study of the internal stratigraphic architecture of the Dragone fan-delta indicates
30 various depositional phases following the main AD 79 alluvial crisis, possibly modulated by
31 the interplay between the availability of loose pyroclastic covers and the varying erosional
32 rates due to the climatic oscillations occurring in the last millennia (Fig. 4; Sacchi *et al.*, 2009;

1 Violante et al., 2009). The major change detectable in the Amalfi fan deltas occurs in the
2 Early Medieval Cool Period (c. AD 500–AD 800), that developed immediately after the
3 Roman Warm Period. Further changes in the stratal patterns of the delta foresets indicative of
4 high streamflow activity, may be correlated with the Medieval Warm Period (c. AD 900–AD
5 1100) and the Little Ice Age (c. AD 1400–AD 1850).

6 **3 Rainstorm-induced geological effects**

7 A field survey was undertaken soon after the 9 September 2010 rainstorm in the Dragone
8 catchment and Atrani village. The observed rainstorm-induced geological effects include:
9 surficial landslides and sediment removal along channels, a temporary dam in the mid-lower
10 section of the Dragone stream, the partial outbreak of the main road crossing the Atrani
11 village, and the deposition of a coarse terminal fan at mouth of the Dragone stream (Fig. 5).

12 The field data indicate that slope erosion triggered by the 9 September 2010 rainstorm was
13 predominantly linear. Sediment removal by linear erosive processes significantly engraved
14 tributaries and the main stream up to a depth of 2 m (Fig. 5A). The displaced materials were
15 mostly composed of pyroclastic deposits and landfills occurring along channel beds often
16 above hydraulic bridges. A large amount of tree trunks of different size mostly coming from
17 rupture of artificial aisles built to cross ditches and tributaries was also included in the
18 transported material.

19 Minor soil slips have been observed uphill on high slope declivity at Punta delle Castagne, a
20 rock crest connecting the S. Eustacchio, S. Caterina, and Scalandrone watersheds (Fig. 5B)
21 and along the western flank of the Frezzi watershed. Here displacement of the channel sides
22 occurred both at channel heads and, locally, in the mid-upper section of small tributaries.

23 Apart overspill deposits composed of white pumices observed at break-slopes just below the
24 watershed areas and along the middle section of the Dragone stream, no significant
25 aggradation has been observed in the catchment area. Removal of materials from stream bed
26 was produced by a fast-moving debris torrent with high erosive capacity, transporting the
27 mobilized materials all the way down to the coast. Here the Dragone stream is artificially
28 forced to flow underneath the main road crossing the Atrani village resulting in siphoning and
29 consequent outbreak of the above roadway (Fig. 5C). Once reached the coastline, the
30 hyperconcentrated flow engraved the Atrani beach and dumped the transported materials at
31 sea in the form of a coarse alluvial fan (Fig. 5E). This induced a shore progradation of about
32 30 m. The alluvial deposits entering into the sea were mostly composed of white-gray

1 pumices including tree trunks, ~~man-made materials, landfills~~, and rock boulders of different
2 size. Some cars parked along the main road were transported up to the beach area and beyond
3 (Fig. 5E).

4 Discharge and depth of flow downstream was probably increased by abrupt draining of a
5 temporary dam reported by eyewitnesses in the lower section of the Dragone stream. Such
6 damming was favoured by a narrow flow section and enhanced by a man-made structure built
7 in the stream bed (Fig. 5D). Failure of temporary debris dams and draining of ephemeral lakes
8 have been described for different flood events occurred in the study area (Passerini, 1924;
9 Penta et al., 1954). ~~This~~ phenomena can produce exceptional temporary discharges and highly
10 destructive peak flows reaching depths as high as 8–10 m (Larsen et al., 2001; Perez, 2001;
11 Esposito et al., 2004a,b; Violante, 2009).

12 **4 Synoptic description and physical features of the meteorological event**

13 **After a sudden summer's interruption at the end of August,** the first days of September 2010
14 in the Mediterranean area were characterized by a drastic seasonal transition. The first
15 depression from the Atlantic was favoured by the formation of an high latitudes anticyclone
16 over Scandinavia. Such anticyclone forced the oceanic perturbed airstream towards medium
17 European latitudes and the Italian peninsula. The unsettled air of Atlantic origin headed later
18 for the ~~basin of~~ low Tyrrhenian where very humid airstreams coming from South/South-West
19 were forced by an area of low pressure centred in northern Tyrrhenian sea. ~~The~~ unstable
20 scenario ~~were~~ fed by the Mediterranean Sea, which created conditions for a secondary area of
21 low pressure to develop in the lower layers of atmosphere.

22 The front was followed on 9 September 2010 by a far more organised instability in the
23 southern Tyrrhenian with well-defined storm cells localized along the Campania, Sicily and
24 Calabria ~~coastal area~~. The high humidity associated with such a positive vorticity lead to a
25 mesoscale convective system (Fujita, 1986) over the southern Tyrrhenian Sea and ~~south~~ Italy,
26 as captured by meteosat image in the visible channel at 17:00 UTC (time hereafter expressed
27 in UTC) on 9 September in Europe (Fig. 6A). The warm-humid flow associated with this
28 system hit the Campania region inducing a strong maritime thunderstorm ~~occurred~~ between
29 10:00 and 22:00 with maximum intensity on the ~~Mt.~~ Lattari as shown in the map of ground
30 **fulminations** (Fig. 6B).

31 The character of the convective system was conditioned by the ~~Mts.~~ Picentini and Lattari that
32 forced the air masses to follow the orography of the coastal range (see Fig. 1) and by positive



1 anomalies of the coastal waters. Data from Italian Oceanographic Network (ISPRA) indicate
2 that the sea-surface temperature in the coastal marine area was 24.8 °C at 14:00 on 9
3 September (Fig. 7A) while higher temperatures exceeding 27 °C for many days were recorded
4 in July and August (Fig. 7B). In Ravello (390 m a.s.l.), Agerola (840 m a.s.l.), and Salerno
5 (16 m a.s.l.) meteo stations (Tab. 1; see also Fig. 3 for location of Ravello gauge station) air
6 temperatures at 14:00 on September 9 were 20.3 °C, 17.7 °C and 22.3 °C respectively. In
7 Salerno the air temperature was 2.5 °C lower than the sea water temperature and decreased
8 abruptly by 6°C in 4 hours and 40 minutes (from 23.7 °C at 13:10 to 17.7 °C at 17:50), in
9 concomitance with the 9 September event. Similar pattern was observed in Ravello (from
10 20.4 °C at 14:30 to 15.4 °C at 17:20) and in Agerola (from 19.1 °C at 13:10 to 13.5 °C at
11 18:10). These data indicate that air temperature was lower than sea-surface temperature
12 during the 9 September rainstorm, maintaining the thermodynamic conditions that allowed the
13 convective system to sustain the storm cell.

14 Physical analysis of the rainstorm was based on the real-time data recorded by rain-gauge
15 stations provided by Centre for weather forecast and monitoring of the Campania Region
16 (Biafiore et al., 2010; Tab. 1). At coast the rainfall lasted 4 hours and started at 14:10 east of
17 Salerno (Fig. 8). In Ravello rain gauge station located along the watershed of the Dragone
18 basin, the rain started at 15:50 and persisted for about 1 hour (cumulative rainfall 80.8 mm)
19 with the maximum rainfall intensity of 116,4 mm (19.4 mm over 10 minutes; Tab. 1) occurred
20 from 15:50 to 16:00. In the Agerola weather station located at about 5 km from the Dragone
21 basin the same event lasted about 1 hour as well with an intensity rainfall peak of 157.2 mm
22 h⁻¹ from 16:00 to 16:10, showing a significant similarity with the cumulative rainfall of the
23 Ravello gauge station (see Fig. 8). This suggest that the Atrani event is consistent with a
24 storm cell characterized by a very limited areal extents as confirmed by Meteosat visible
25 image that show a single cell with a very flat elliptical shape that elongates in NE-SW
26 direction (inset in Fig. 6A).

27 The size of the storm cell that produced the Atrani event was calculated: 1) by considering the
28 50 mm isohyet corresponding to the down-draft in the time-span ranging from 16:00 to 16.50
29 (Fig. 9); 2) on the base of the number of pixels forming the storm cell visible in the MeteoSat
30 images at 17:00. In the first case the area was about 80 km²; in the latter the area was ranging
31 from 56 to 75 km². Therefore, the Atrani storm cell can be ascribed to a Mesoscale
32 Convective System - MCS with an horizontal scale of about 20-30 km and duration lower

1 than an hour (lower bound of the MCS mesoscale β ; Orlansky, 1975; Thunis and Borstein,
2 1996). These events typically occur in the Mediterranean Sea between April and September,
3 with a higher frequency mostly concentrated during September (Lionello et al., 2006) and
4 include multiple storm cells in different evolutionary stages (Morel and Senesi, 2002) that are
5 strongly influenced by local orography.

6 **5 Hydrological model**

7 In order to evaluate the hydrological response of the Dragone basin at the stream mouth a
8 semi-distributed rainfall-runoff model has been used. For this aim each of the 5 sub-basins of
9 the Dragone stream (see Fig. 3A and Tab. 2) were analyzed by Soil Conservation Service
10 (SCS) dimensionless unit hydrograph rainfall-runoff transformation, and SCS Curve Number
11 (CN) loss method (USDA SCS, 1986a) implemented in HEC-HMS (USACE HEC, 2010).

12 The SCS dimensionless unit hydrograph procedure is one of the most well known methods for
13 deriving synthetic unit hydrographs, especially for small basins. The rainfall-runoff model is
14 based on the lag time parameter, that is the time interval between the centroid of the effective
15 rainfall hyetograph and the peak of discharge (Tab. 3; Singh, 1989; USDA SCS, 1986b).

16 The effective precipitation depth, according to the SCS-CN procedure, is:

$$17 \quad P_e = \begin{cases} \frac{(P - I_a)^2}{(P - I_a + S)} & \text{if } P > I_a \\ 0 & \text{if } P \leq I_a \end{cases} \quad (1)$$

18 Where P is the total precipitation depth, P_e is the depth of excess precipitation or direct
19 runoff, I_a is the “initial abstraction” or the amount of rain before the runoff starts, which
20 infiltrates or is intercepted by vegetation, S is the potential maximum soil moisture retention
21 during the runoff.

22 The value of S for a given soil is related to the curve number (CN) which is function of the
23 hydrologic soil-cover complexes as (if S is expressed in mm):

$$24 \quad CN = \frac{25400}{S + 254} \quad (2)$$

25 In the case of the Dragone basin the adopted CN value is 66 corresponding to forest-like
26 cover (woods-grass combination), considering hydrological soil group B (moderate
27 infiltration) with antecedent moisture condition II (average) and $I_a = 0.2 S$.

1 The lag time t_{lag} has been estimated from concentration time t_c calculated by SCS formula
2 (Chow et al., 1988):

$$3 \quad t_{lag} = 0.6 \times t_c = 0.6 \times 0.00227 \times L^{0.8} \left(\frac{1000}{CN} - 9 \right)^{0.7} i^{-0.5} \text{ [hour]} \quad (3)$$

4 Where L is the hydraulic watershed length expressed in meter (m) and i the mean basin slope
5 as percentage (%). Figure 10 reports the results of the hydrological model where the estimated
6 peak discharge of the clear water is about $65 \text{ m}^3 \text{ s}^{-1}$ occurring around the 17:00.

7 **6 Hydraulic model and sediment transfer**

8 Due to the lack of streamgauge data, we analyzed the hydraulic response of Dragone
9 catchment to the 9 September 2010 rainstorm event and the sediment transfer during flood on
10 the base of (a) morphology of the Dragone basin; (b) pluviometric data; (c) field evidences;
11 (d) homemade-videos and photos; (e) eyewitnesses accounts.

12 According to local eyewitness accounts, the peak flow of the Atrani flood event occurred
13 between 16:50 and 17:10, that is about 40 minutes later of the hyetograph centroid, occurred
14 at ca 16:25, while the flood duration was ranging from 40 to 60 minutes (Fig. 11). In the
15 Atrani urban area the entombment of the Dragone stream splitted the flood wave in two
16 different currents: a main flow within the entombment, below the road level (“via Dei Dogi”)
17 along a closed section varying from $3(h) \text{ m} \times 9(w) \text{ m}$ at input section to $1.80(h) \text{ m} \times 5.50(w)$
18 m at closing section; a second flow above the entombment, along the road, constrained by
19 almost continuous man-made structures and buildings 5.5 m away from each others (see Fig.
20 5 C). The maximum depth of the upper flow was about 1 m, meaning around 3.5 m on
21 average from the stream bed.

22 The highest flow velocity for both flows was estimated from amateur videos by tracking
23 particles transported by the flood through the analysis of video frames with an approach
24 similar to that used in PIV technique (Fig. 12; Raffel et al., 2007). Peak discharge is obtained
25 by multiplying estimated flow velocity and the flow section.

26 The estimated flow velocity along via Dei Dogi street is about $3\text{-}4 \text{ m s}^{-1}$ and, consequently,
27 the peak discharge is approximately $20 \text{ m}^3 \text{ s}^{-1}$. For the entombed flow the estimated peak
28 velocity is about $6\text{-}7 \text{ m s}^{-1}$ while the peak discharge is in the order of $60 \text{ m}^3 \text{ s}^{-1}$, taking into
29 account that the flow fills roughly the 80% of the closed section. Then the total estimated
30 peak discharge is $80 \text{ m}^3 \text{ s}^{-1}$ (water + sediment; see Fig. 11), which is $15 \text{ m}^3 \text{ s}^{-1}$ more than the

1 estimated clear water peak discharge ($65 \text{ m}^3 \text{ s}^{-1}$) due to sediment load (Q_s). Similar values for
2 total peak discharge ($98.4 \text{ m}^3 \text{ s}^{-1}$) has been reported by Ciervo et al., 2014 that used a
3 dedicated numerical code for the hydraulic modelling of the 9 September 2010 Atrani flash
4 flood.

5 Assuming that active sediment removal occurred in a time span of 40÷60 minutes, the
6 calculated sediment volume mobilized during the event is:

$$7 \quad V_s = Q_s \times t = 15 \times \frac{(40 \div 60)}{2} \times 60 = 18000 \div 27000 \text{ m}^3 \quad (4)$$

8 This value is in good agreement with volume estimation of the sediment deposited in the form
9 of alluvial fan delta at the Dragone mouth and on the street and square that cover the the
10 stream path (Fig. 13). To this aim, bathymetric data collected soon after the flood event were
11 compared with an older dataset owned by IAMC_CNR enabling the measurement of sediment
12 volume that flowed into the sea at ca 14000 m^3 (Fig. 13). On land, sediment thickness along
13 via Dei Dogi and Umberto I square reached depths averaging 0.5 m while beach aggradation
14 was about 1m, with a volume of sediment accumulation of ca 7000 m^3 . Therefore, the
15 estimated volume of the sediment transported to the terminal section of the Dragone stream is
16 ca 21000 m^3 . Taking into account the additional volumes (estimated at about 20% of the
17 measured volume) removed by sea currents or related to dispersal of finer sediments at sea, a
18 total volume of about 25000 m^3 can be obtained.

19 Sediment volume can be expressed as sediment bulking factor (BF; Gusman et al., 2009) that
20 define the ratio between the peak flood discharge Q_B and clear water discharge (Q_w):

$$21 \quad BF = \frac{Q_B}{Q_w} = \frac{Q_w + Q_s}{Q_w} \quad (5)$$

22 In terms of sediment load, bulking factor can be also expressed as:

$$23 \quad BF = \frac{1}{1 - \frac{C_V}{100}} \quad (6)$$

24 Where C_V is the volume concentration of sediment.


25 In the case of the 9 September 2010 flood event the estimated BF to the flood peak is 1.2 (5)
26 that leads to a sediment concentration in the order of 20% in volume (6). This value is close to
27 the lower limit of hyperconcentrated flow (Costa, 1988; Jakob and Hungr, 2005) and it
28 corresponds to a flow in which peak discharge is comparable to that of a clear water flood and

1 velocities are similar to those of water during a flood (Hungry et al., 2001; Pierson, 2005). This
2 is also confirmed by amateur videos that show a very turbulent flow.

3 **7 Historical documentation of past floods**

4 A systematic analysis of documentary and bibliographic sources, as well as newspapers
5 carried out at the State Archives in Naples and Salerno (Esposito et al., 2003; 2004; Porfido et
6 al., 2009), complemented by data attained from scientific papers and national and
7 international projects (Guzzetti et al., 1994; Guzzetti and Tonelli, 2004) allowed us to
8 reconstruct the time-space distribution of flood events that have affected Atrani since 1540.
9 The quality and completeness of the various sources were evaluated and carefully analyzed in
10 their historical context, to obtain the best information rather than the best dataset quality
11 (Barriandos et al., 2003). Nineteen events were identified and characterized on the basis of: a)
12 distribution of the flooded areas, b) distribution of damaged localities, c) duration and timing
13 of the event and d) number of casualties. The historical information show that most of the
14 events (14 events) took place at season transition between summer and autumn, four events in
15 winter and just one has been recorded into the spring season (Tab. 4).

16 The intensity and the duration of the rainfalls, the level and distribution of damage of man-
17 made structures, the number of victims, and the induced geological effects have been
18 considered to distinguish flash flood from minor flood types (Tab. 4; Casas Planes et al.,
19 2003; Llasat et al., 2005; Barnolas & Llasat, 2007). In particular, shoreline progradation has
20 been considered as a key element for flash-flood as it results from bed load transport and
21 hyperconcentrated stream-flows. Based on this, 7 flood events out of 19 have been classified
22 as flash flood:

- 1 • October 1540 - Not much information are available for this event, but it is reported as
2 “the great Atrani flood”. This indication along with the occurrence of severe damage
3 and extensive landslides and inundation allow to classify it as a flash flood.
- 4 • August 1588 - A flood produced severe damage to properties, extensive inundation,
5 landslides and shoreline progradation, as reported by the Cronaca Amalphitana, Ignoti
6 auctoris 1588, cited by Camera (1881): “at the end of the past month of August 1588
7 much lava fell down. . . it destroyed the Seggio building. . . the force of the lava
8 removed trees, wood, earth and rocks and . . . it filled the harbor and pushed the sea
9 back seven roads (14 m) thereby enlarging the harbor”.
- 10 • 20 January 1764 - A flood caused much damage to the Santa Maria Acquabona
11 Church and to many flour mills as well as to some bridges. Extensive landslide 
12 coming from Scala hit Atrani, causing two deaths. The sediment transfer from Scala to
13 Atrani indicates a mass transport along the main stream likely produced by a flash
14 flood.
- 15 • 17 January 1780 - Heavy rain hit the Atrani village causing 26 casualties, a huge
16 landslide and extensive damage (Greco, 1787). The elevated number of victims
17 suggest a flash flood event.
- 18 • 18 August 1949 - On August 18, water masses flooded along the Atrani main street
19 and square, reaching ~~the level~~ of about three meters. A widespread pattern of
20 destruction characterized this event: boats, nets, fishing gear were swept away or
21 submerged by mud; damage to buildings, destruction of roads, aqueducts and sewer
22 systems. Thousands of cubic meters of material and muddy debris were left in the
23 Umberto I square as well as on the beach producing a shoreline progradation of about
24 20 m.
- 25 • 1 October 1949 The effects of the past flood event were still evident when a second
26 one occurred with a greater violence. Outbreak of the main street occurred in several
27 places, and water supply pipelines, recently refitted, were destroyed again. Huge
28 amounts of debris and mud were transported all the way down to the coast in addition
29 to the material recently transported by the 18 August flood, so that a large beach
30 developed at the foot of coastal cliffs in between the Atrani village and the nearby
31 locality of Castiglione.

1 8 Conclusions

2 Detailed field surveys and measurements along with information from eyewitnesses and
3 amateur videos proved to be critical for modelling and reconstruct the flash flood that affected
4 the Atrani village on 9 September 2010. The collected data were combined with
5 meteorological and historical analyses and marine geophysical surveys in order to reconstruct
6 the physical features of the flood event and the recurrence of flash-flood in the study area. The
7 main results can be summarized as follows:

- 8 • The rainstorm that generated the Atrani event lasted 4 hours and was strongly
9 conditioned by the local orography and positive thermic anomalies of the coastal
10 waters during the warm season.
- 11 • In Atrani the rainfall event lasted about 1 hour with cumulative rainfall of 80.8 mm
12 and maximum rainfall intensity nearly to 120 mm h^{-1} . It was produced by a single
13 storm cell elongated in NE-SW direction with a very flat elliptical shape and of
14 limited areal extent (from 50 to 70 km^2) that can be ascribed to a Mesoscale
15 Convective System β type.
- 16 • The estimated peak discharge of the clear water produced in the Dragone stream is
17 about $65 \text{ m}^3 \text{ s}^{-1}$ while the estimated total peak discharge (water + sediment) is $80 \text{ m}^3 \text{ s}^{-1}$
18 leading to a sediment concentration of about of 20% in volume characteristic of a
19 debris flood.
- 20 • Sediment removal mostly occurred through linear erosion that significantly engraved
21 tributaries and the main stream. The displaced materials were mostly composed of
22 pyroclastic deposits and landfills occurring at channel beds and behind hydraulic
23 bridges. A reduced size of erodible sediment stored in channels may consequently
24 reduce mud-flow hazard and provide protection for the residential area on the alluvial
25 fan in Atrani.
- 26 • The analysis of historical sources shows that 19 flood events occurred in the Dragone
27 catchment in the last five centuries. Of these 7 events were classified as flash-flood
28 and 12 as minor flood. The internal stratigraphic architecture of the Dragone fan-delta
29 confirms the recurrence of flooding event in the Early Medieval Cool Period (c. AD
30 500–AD 800), in the Medieval Warm Period (c. AD 900–AD 1100) and the Little Ice
31 Age (c. AD 1400–AD 1850).

1 The approach used in this work is representative of geomorphological and urban contexts
2 characterized by very small ungauged and rocky watersheds with ephemeral discharge and
3 local communities mostly living at stream mouths. In these settings the importance of
4 erosional processes claim the use of different data sources for predictive water models that
5 include geological and hydrological analyses.


6 **Acknowledgements**

7 The authors wish to thank Crescenzo Minotta, geologist at Autorità di Bacino Campania Sud,
8 and Maria Carla Sorrentino archaeologist and member of the Centro Universitario Europeo
9 per i Beni Culturali for support with post-event bathymetric survey and assistance in the field
10 respectively. We also thank Luigi Amato of the Cultural Association “Sos Dragone” that
11 helped to reconstruct the timing of the flooding event. This work was founded by a research
12 grant P0000274 to Crescenzo Violante.

13

1 **References**

- 2 Barnolas, M. and Llasat, M. C.: A flood geodatabase and its climatological applications: the
3 case of Catalonia for the last century, *Nat. Hazards Earth Syst. Sci.*, 7, 271-281,
4 doi:10.5194/nhess-7-271, 2007.
- 5 Barriendos, M., Llasat, M. C., Barrera, A. and Rigo, T.: The study of flood events from
6 documentary sources, *Methodological guidelines for historical sources identification and*
7 *flood characterization in the Iberian Peninsula*, in: *Palaeofloods, Historical Floods and*
8 *Climatic Variability: Applications in Flood Risk Assessment (Proceedings of the Phefra*
9 *Workshop, Barcelona, 16–19 October, 2002)*, edited by: Thorndycraft, V. R., Benito, G.,
10 Barriendos, M., and Llasat, M. C., 87–92, 2003
- 11 Biafiore M. et alii: Rapporto dell'evento del 9 settembre 2010 nel territorio dei Comuni di
12 Atrani e Scala, Centro Funzionale per la previsione meteorologica e il monitoraggio meteo-
13 pluvio-idrometrico e delle frane (Regione Campania), 38 pp., 2010.
- 14 Budillon, F., Violante, C., Conforti, A., Esposito, E., Insinga, D., Iorio, M. and Porfido, S.:
15 Event beds in the recent prodelta stratigraphic record of the small flood-prone Bonea Stream
16 (Amalfi Coast, Southern Italy), *Marine Geology*, 222–223, 419–441, 2005
- 17 Camera, M.: *Memorie storico diplomatiche dell'antica città e ducato di Amalfi*, pp. 80, 1881,
18 reprinted Centro Cultura e Storia amalfitana, Amalfi 1999.
- 19 Casas Planes, A., Benito, G., D'íez Herrero, A. and Barriendos, M.: *Sphere-Gis:*
20 *Implementation of an historical and palaeoflood geographical information system*, in:
21 *Palaeofloods, Historical Floods and Climatic Variability: Applications in Flood Risk*
22 *Assessment (Proceedings of the Phefra Workshop, Barcelona, 16th–19th October, 2002)*,
23 edited by: Thorndycraft, V. R., Benito, G., Barriendos, M. and Llasat, M. C., 363–368, 2003.
- 24 Chow, V.T., Maidment, D.R. and Mays, L.W. (Eds). *Applied Hydrology*, McGraw Hill New
25 York, 572 pp., 1988.
- 26 Ciervo F., Papa M. N., Medina V., Bateman A.: Simulation of flash floods in ungauged basins
27 using post-event surveys and numerical modelling. *Journal of Flood Risk Management*, 1-13,
28 2014.
- 29 Cinque, A. and Robustelli, G.: Alluvial and coastal hazards caused by long-range effects of
30 Plinian eruptions: the case of the Lattari Mts. After the AD 79 eruption of Vesuvius, in:

- 1 Geohazard in Rocky Coastal Areas, edited by: Violante C., Geological Society of London,
2 Special Publications, 322, 155–171, doi:10.1144/SP322.7, 2009.
- 3 Costa, J.E.: Rheologic, geomorphic, and sedimentologic differentiation of water floods,
4 hyperconcentrated flows, and debris flows, in: Flood Geomorphology edited by: Baker, V.R.,
5 Kochel, R.C., and Patten, P.C., Wiley-Intersciences, New York, 113-122, 1988.
- 6 Esposito E., Porfido S., Violante C. and Alaia F.: Disaster induced by historical floods in a
7 selected coastal area (southern Italy), in: Palaeofloods, Historical Floods and Climatic
8 Variability: Applications in Flood Risk Assessment (Proceedings of the Phefra Workshop,
9 Barcelona, 16–19 October, 2002), edited by: Thorndycraft, V. R., Benito, G., Barriendos, M.,
10 and Llasat, M. C., 143–148, 2003.
- 11 Esposito, E., Porfido, S. and Violante, C. (Eds): Il Nubifragio dell'Ottobre 1954 a Vietri sul 
12 Mare, Costa d'Amalfi, Salerno. Scenario ed effetti di una piena fluviale catastrofica in un'area
13 di costa rocciosa, GNDICI, 2870, ISBN: 88-88885-03-X, 380 pp., 2004a.
- 14 Esposito, E., Porfido, S., Violante, C., Biscarini, C., Alaia, F. and Esposito, G.: Water events
15 and historical flood recurrences in the Vietri sul Mare coastal area (Costiera Amalfitana,
16 southern Italy), in: The Basis of Civilization—Water Science?, edited by: Rodda, G. and
17 Ubertini, L., International Association of Hydrological Sciences Publication, 286, 1–12,
18 2004b.
- 19 Fujita, T. T.: Mesoscale classifications: their history and their application to forecasting, in:
20 Mesoscale Meteorology and Forecasting, edited by: Ray, P. S., American Meteorological
21 Society, Boston, 18-35, 1986.
- 22 Greco, M.: Cronaca di Salerno. Reprinted Palladio Salerno. 1787.
- 23 Gusman, A.J., Teal, M.J., Todesco, D. and Bandurraga, M.: Estimating Sediment/Debris
24 Bulking Factors, in: Proceeding of 33rd IAHR Congress, Vancouver, British Columbia,
25 Canada 9-14 August 2009, 83-91, ISBN: 978-1-61738-231-4, 2009.
- 26 Guzzetti, F., Cardinali, M. and Reichenbach, P.: The AVI Project: A bibliographical and
27 archive inventory of landslides and floods in Italy, Environ. Manage., 18(4), 623-633, 1994.
- 28 Guzzetti, F. and Tonelli, G.: Information system on hydrological and geomorphological
29 catastrophes in Italy (SICD): a tool for managing landslide and flood hazards, Nat. Hazards
30 Earth Syst. Sci., 4, 213–232, 2004.

- 1 Hungr, O., Evans, S.G., Bovis, M., and Hutchinson, J.N.: Review of the classification of
2 landslides of the flow type, *Environmental and Engineering Geoscience*, 7, 221-238, 2001.
- 3 Jakob, M. and Hungr, O. (Eds) *Debris Flow Hazards and Related Phenomena*, Springer-
4 Praxis Book in Geophysical Science, Springer-Verlag Berlin Heidelberg N.Y, ISBN 3-540-
5 20726-0, 733 pp., 2005.
- 6 Larsen, M. C., Wieczorek, G. F., Eaton, L. S., Morgan, B. A and Torres-Sierra, H.: Natural
7 hazards on alluvial fans; The Venezuela debris flow and flash flood disaster. US Geological
8 Survey, Fact Sheet, 103-01, 2001.
- 9 Lionello, P., Bhend, J., Buzzi, A., Della-Marta, P.M., Krichak, S., Jansà, A., Maheras, P.,
10 Sanna, A., Trigo, I.F., Trigo, R.: Cyclones in the Mediterranean region: climatology and
11 effects on the environment, in: *Mediterranean Climate Variability*, edited by: Lionello, P.,
12 Malanotte-Rizzoli, P., Boscolo, R., Elsevier, 325-372, ISBN 10-0-444-52170-4, 2006.
- 13 Llasat, M. C., Barriendos, M., Barrera, T., and Rigo, T.: Floods in Catalonia (NE Spain) since
14 the 14th century. Climatological and meteorological aspects from historical documentary
15 sources and old instrumental records, *J. of Hydrol.*, 313, 32-47, 2005.
- 16 Morel, C. and Senesi, S.: A climatology of mesoscale convective systems over Europe using
17 satellite infrared imagery. II: Characteristics of European mesoscale convective systems, *Q. J.*
18 *R. Meteorol. Soc.*, 128, 1973-1995, 2002.
- 19 Orlandy, I.: A rational subdivision of scales for atmospheric processes, *Bull. of the Am.*
20 *Meteorol. Soc.*, 56(5), 527-530, 1975.
- 21 Passerini, G.: *Intorno alle cause del disastro del marzo 1924 nella Penisola Sorrentina*, *Boll.*
22 *Ist. Agrario di Scandicci, Ricerche ed esperienze istituite dal 1914 al 1925*, 8, ISBN: 0366-
23 1881, 249-269, 1925.
- 24 Penta, F., Lupino, R., Camozza, F. and Esu, F.: Effetti dell'alluvione del 26 ottobre 1954 nel
25 Salernitano, *Rivista Italiana di Geotecnica*, 6, 245-257, 1954.
- 26 Perez, F. L.: Matrix granulometry of catastrophic debris flows (December 1999) in central
27 coastal Venezuela, *Catena*, 45, 163-183, 2001.
- 28 Pierson, C.: Hyperconcentrated flow—transitional process between water flow and debris
29 flow, in: *Debris-flow Hazards and Related Phenomena*, edited by: Jakob, M. and Hungr, O,
30 Springer/Praxis, Chichester, UK, 159-202, 2005.

1 Porfido S., Esposito E., Alaia F., Molisso F. and Sacchi M.: The use of documentary sources
2 for reconstructing flood chronologies on the Amalfi rocky coast (southern Italy). in:
3 Geohazard in Rocky Coastal Areas, edited by: Violante C., Geological Society of London,
4 Special Publications, 322, 173–187, doi:10.1144/SP322.8, 2009.

5 Raffel, M., Willert, C.E., Wereley, S.T. and Kompenhans, J.: Particle Image Velocimetry. A
6 Practical Guide, 2nd Ed., Springer Berlin. 447 pp. 2007.

7 Sacchi, M., Molisso, Violante, C., Esposito, E., Insinga, D., Lubritto C., Porfido S. and Toth
8 T. Insights into flood dominated fan deltas: very high-resolution seismic examples off the
9 Amalfi cliffed coasts, eastern Tyrrhenian Sea, in: Geohazard in Rocky Coastal Areas, edited
10 by: Violante C., Geological Society of London, Special Publications, 322, 33–72, doi:
11 10.1144/ SP322.2, 2009.

12 Sigurdsson, H., Carey, S., Cornell W. and Pescatore, T.: The eruption of Vesuvius in AD 79,
13 Nat. Geog. Res., 1, 332–387, 1985.

14 Singh, V. P. (Ed): Hydrologic Systems. Watershed Modelling, Prentice Hall Englewood
15 Cliffs, New Jersey, 1989.

16 Thunis, P. and Bornstein, R: Hierarchy of Mesoscale Flow Assumptions and Equations, J. of
17 Atmos. Sci., 53, 380–397, 1996.

18 USDA-SCS: Technical Release 55: Urban Hydrology for Small Watersheds, USDA (U.S.
19 Department of Agriculture). <http://www.cpsc.org/reference/tr55.pdf>, 1986a.

20 USDA-SCS: National Engineering Handbook, Section 4 - Hydrology. Washington, D.C.,
21 1986b.

22 USACE HEC: Hydrologic Modelling System version 3.5, User's Manual (CPD-74A), 2010.

23 Violante, C.: Rocky coast: geological constrains for hazard assessment, in: Geohazard in
24 Rocky Coastal Areas, edited by: Violante C., Geological Society of London, Special
25 Publications, 322, 1–31. DOI: 10.1144/SP322.1, 2009.

26 Violante, C., Biscarini, C., Esposito, E., Molisso, F., Porfido, S. and Sacchi, M.: The
27 consequences of hydrologic events on steep coastal watersheds: the Costa d'Amalfi, eastern
28 Tyrrhenian sea, in: The Role of Hydrology in Water Resource Management, edited by:
29 Liebsher, H. J. et al., Capri Italy, 2008. IAHS Publication, 327, 102–113, 2009.

1 Table 1. Rainfall intensity (mm) registered at time intervals of 10 minutes and 1 hour on
 2 September 9 2010 by rain gauges in Salerno and Sorrento Peninsula. In bold are reported the
 3 maximum values. Data from Centre for weather forecast and monitoring of the Campania
 4 Region (Biafiore et al., 2010).

Rain gauge	Altitude (m)	Latitude	Longitude	Distance from Ravello (km)	Rainfall intensity (mm)	
		N	E		10'	1h
Pontecagnano	36	40° 38' 36.9"	14° 52' 02.2"	21,8	15,0	53,6
Salerno Meteo	16	40° 38' 37.7"	14° 50' 11.5"	20,3	16,0	47,0
Ravello	390	40° 39' 24.3"	14° 36' 52.5"	0,0	19,4	80,8
Agerola Meteo	848	40° 38' 48.6"	14° 32' 26.2"	6,0	26,2	80,8
Agerola	623	40° 38' 21.3"	14° 32' 44.8"	5,7	21,6	66,8
Moiano	485	40° 39' 12.6"	14° 27' 50.0"	13,5	21,0	78,0
Pimonte	437	40° 40' 27.8"	14° 30' 17.4"	10,2	23,2	92,2
Maiori	10	40° 39' 05.7"	14° 38' 24.6"	3,0	12,0	43,0
Gragnano	195	40° 41' 15.1"	14° 31' 38.1"	8,6	14,8	70,0
Lettere	312	40° 42' 15.9"	14° 31' 58.3"	9,8	16,2	45,6
Corbara	424	40° 43' 32.8"	14° 36' 07.5"	9,1	18,4	45,0
Tramonti	422	40° 42' 13.9"	14° 38' 49.3"	6,9	12,4	42,6
Amalfi	114	40° 37' 23.7"	14° 34' 49.8"	1,4	11,0	28,6
Cetara	140	40° 39' 04.0"	14° 42' 12.5"	8,6	9,8	27,2

5
6
7
8
9
10
11
12
13
14
15
16

1 Table 2 - Main morphometric parameters used in the hydrologic model.

Sub-basin	Name	A (km ²)	L (m)	S (%)	H _{mean} (m a.s.l.)	H _{min} (m a.s.l.)
Basin_1	Scalandrone	1.39	3600	56.7	873	389
Basin_2	Nocelle	1.46	2450	60.5	922	479
Basin_3	Frezzi	2.66	2600	54.3	803	479
Basin_4	Senite	1.12	1000	46.7	570	389
Basin_5	Sant'Eustacchio	2.71	3200	60.3	411	0
Whole basin	Dragone	9.33	6800	56.5	692	0

2
3
4
5
6
7
8
9
10
11
12
13
14
15
16
17
18
19
20

1
2
3
4
5
6
7
8
9
10
11
12
13
14
15
16
17
18
19
20

Table 3 - Estimated lag-time values e CN parameter used in the hydrologic model.

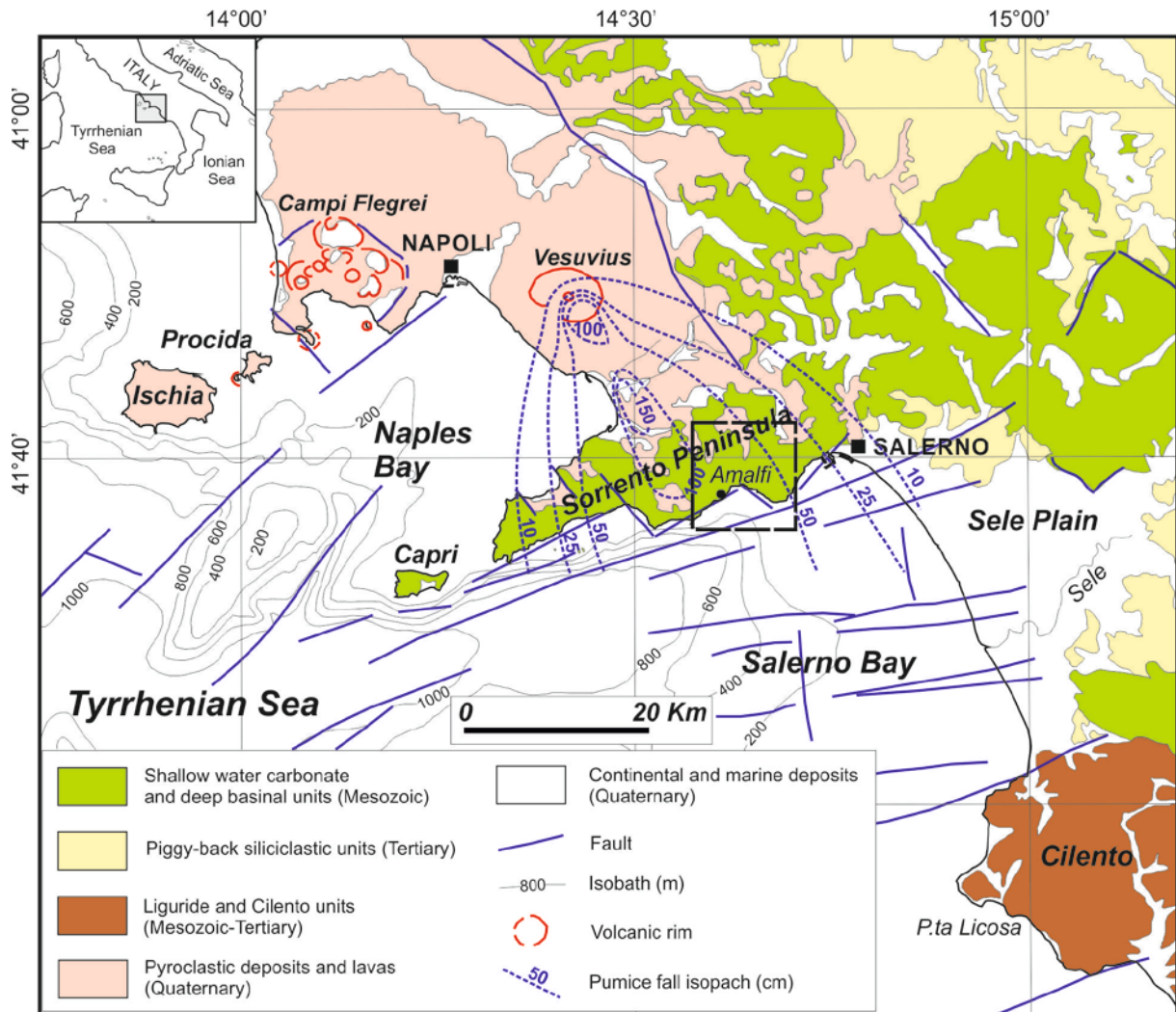
Sub-basin	CN (-)	t _c (minutes)	t _{lag} (minutes)
Basin_1	66	44	26
Basin_2	66	32	19
Basin_3	66	34	20
Basin_4	66	17	10
Basin_5	66	38	23
Whole basin	66	72	43

1 Table 4 – Flood events occurred at Atrani from 1540 to 2010 with indication of the induced
 2 effects. FF: Flash-flood. MF: Minor flood.

Year	Month	Day	Damage	Victims	Geological Effect	Flood Type
1540	10	8	Severe	-	Slides	FF
1588	8	31	Major	Some	Shoreline progradation	FF
1764	1	20	Major	2		FF
1780	1	17	Severe	26		FF
1823	10	18	Minor			MF
1824	10	3	Minor			MF
1904	10	7	Minor			MF
1924	3	27	Minor		Slides	MF
1935	3	1	Minor			MF
1949	8	18	Major		Shoreline progradation	FF
1949	10	1	Major		Shoreline progradation	FF
1953	9	11	Minor			MF
1954	10	25	Minor			MF
1969	3	15	Minor			MF
1984	8	28	Minor	1		MF
1987	10	6	Minor			MF
1988	9	14	Minor			MF
2007	9	20	Minor			MF
2010	9	10	Severe	1	Shoreline progradation	FF

3
 4
 5
 6
 7
 8
 9
 10
 11

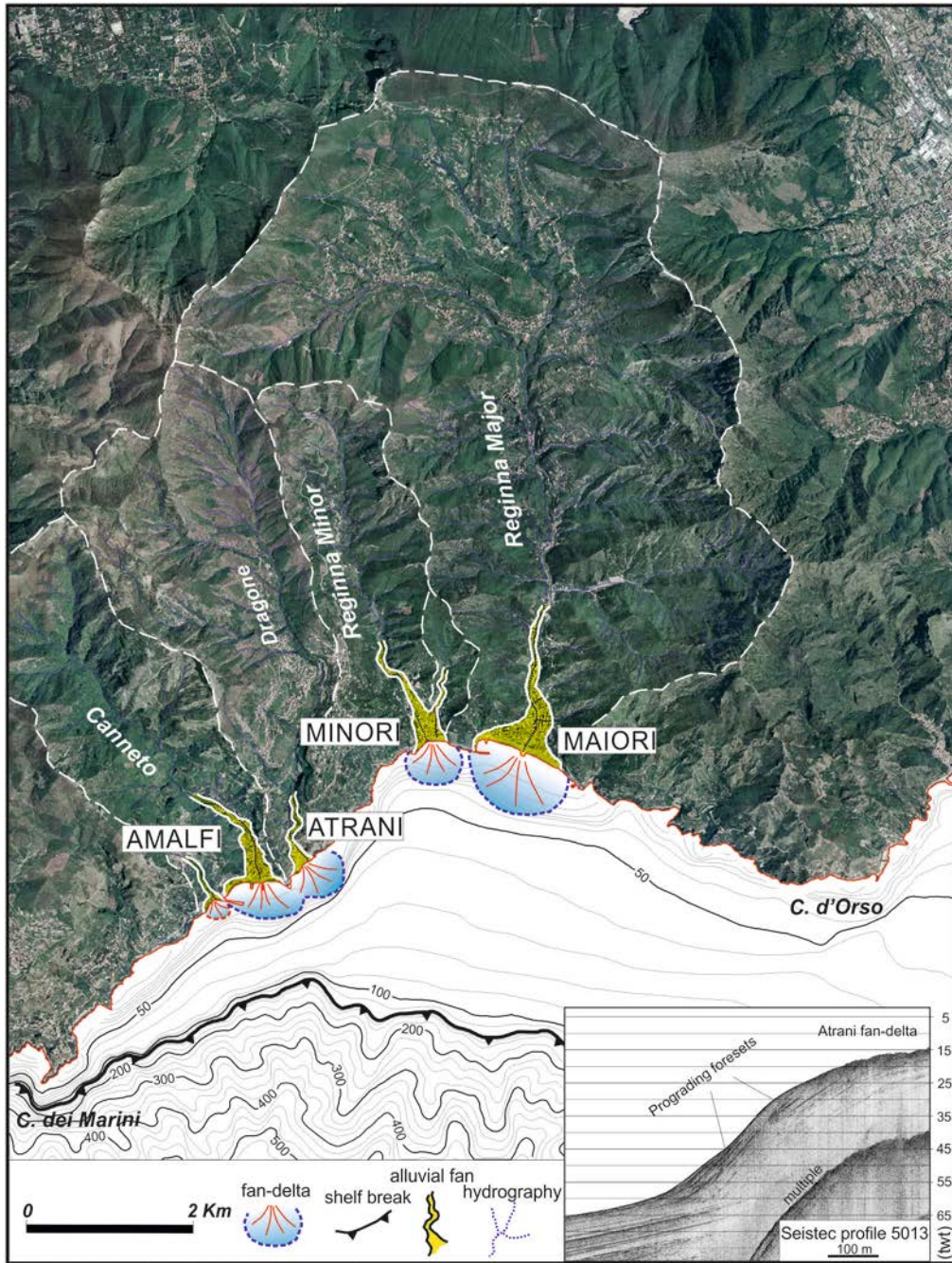
1 Figure 1



2
3
4
5
6
7
8
9
10
11
12

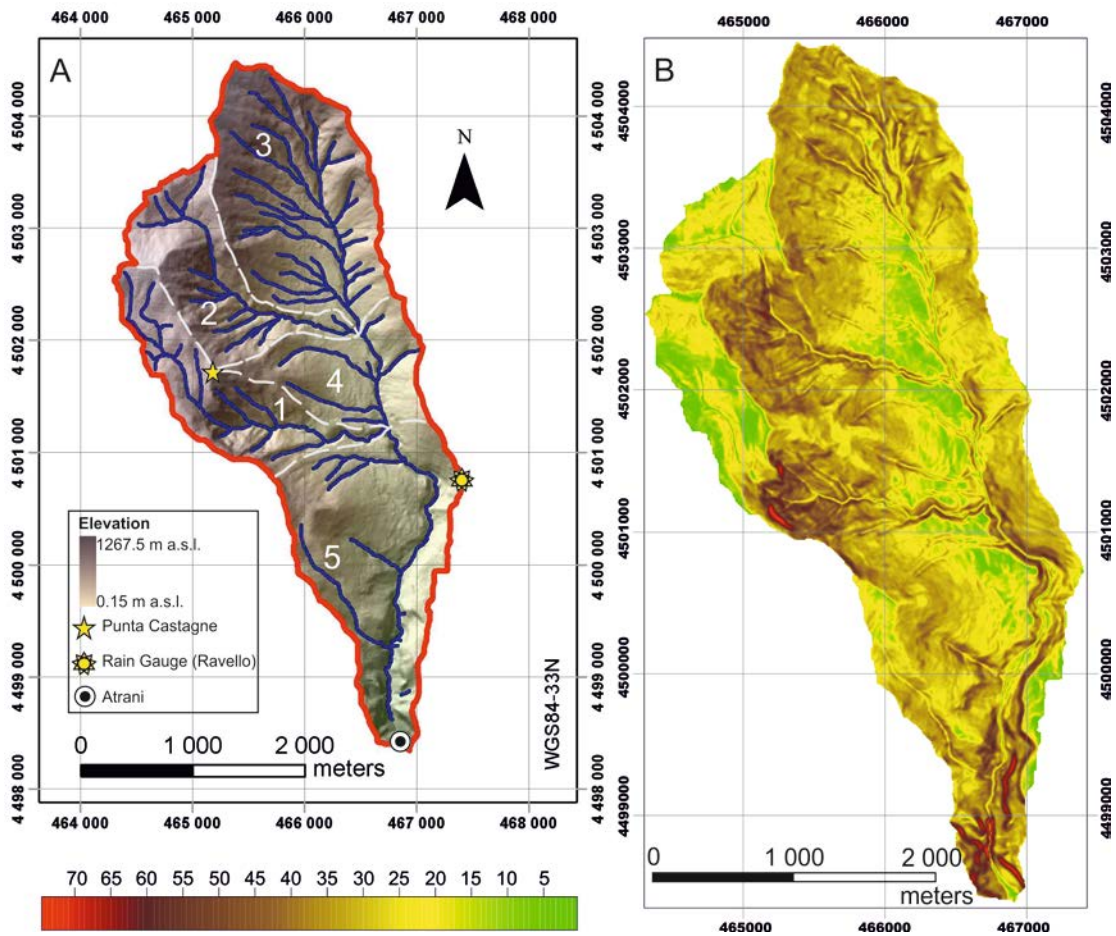


1 Figure 2



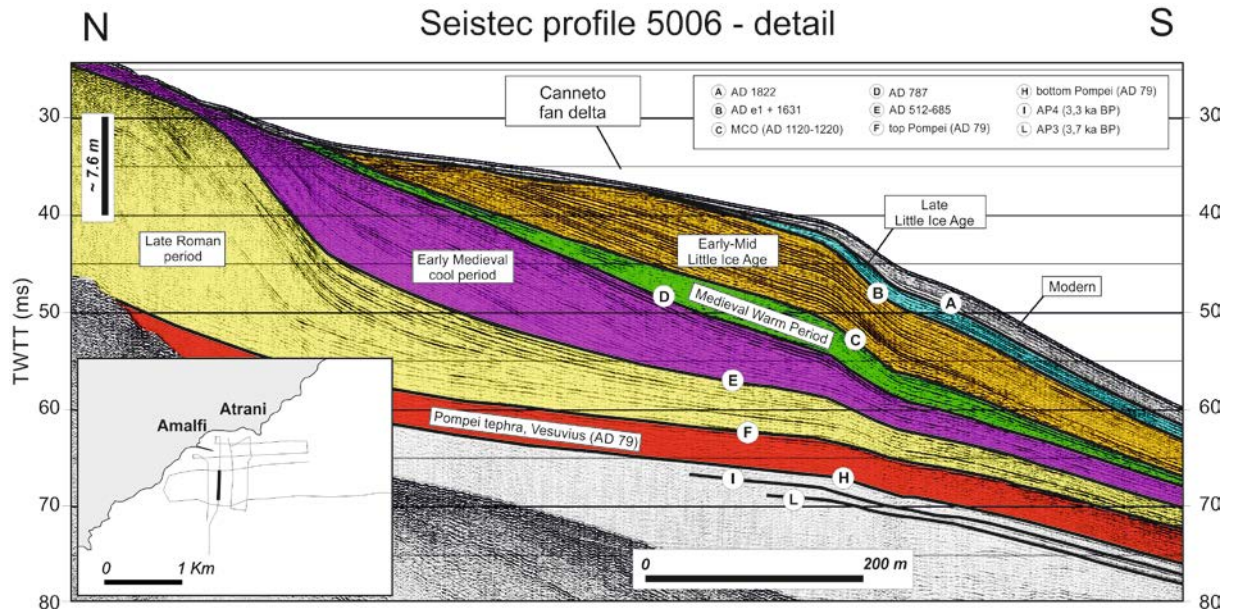
2
3
4
5
6
7

1 Figure 3



- 2
- 3
- 4
- 5
- 6
- 7
- 8
- 9
- 10
- 11
- 12
- 13

1 Figure 4



- 2
- 3
- 4
- 5
- 6
- 7
- 8
- 9
- 10
- 11
- 12
- 13
- 14
- 15
- 16
- 17
- 18

1 Figure 5



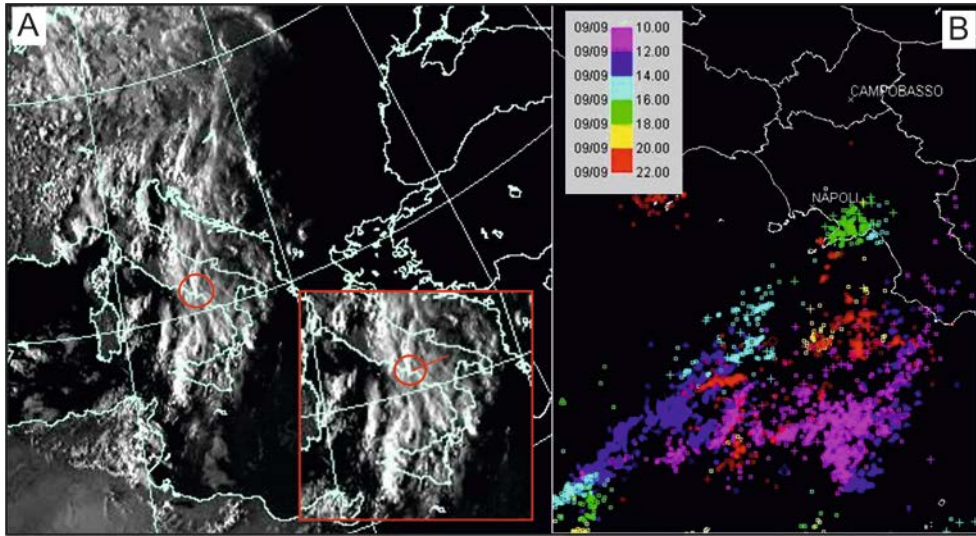
2

3

4

5

1 Figure 6



2

3

4

5

6

7

8

9

10

11

12

13

14

15

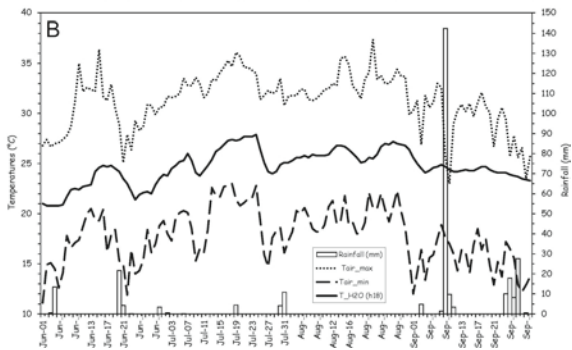
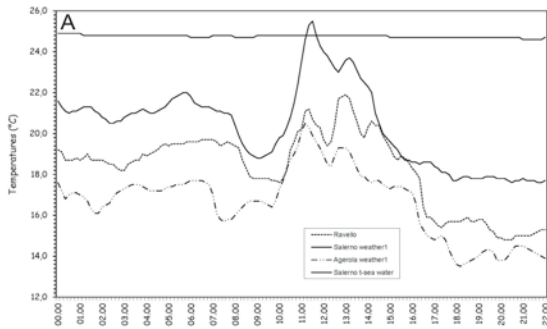
16

17

18

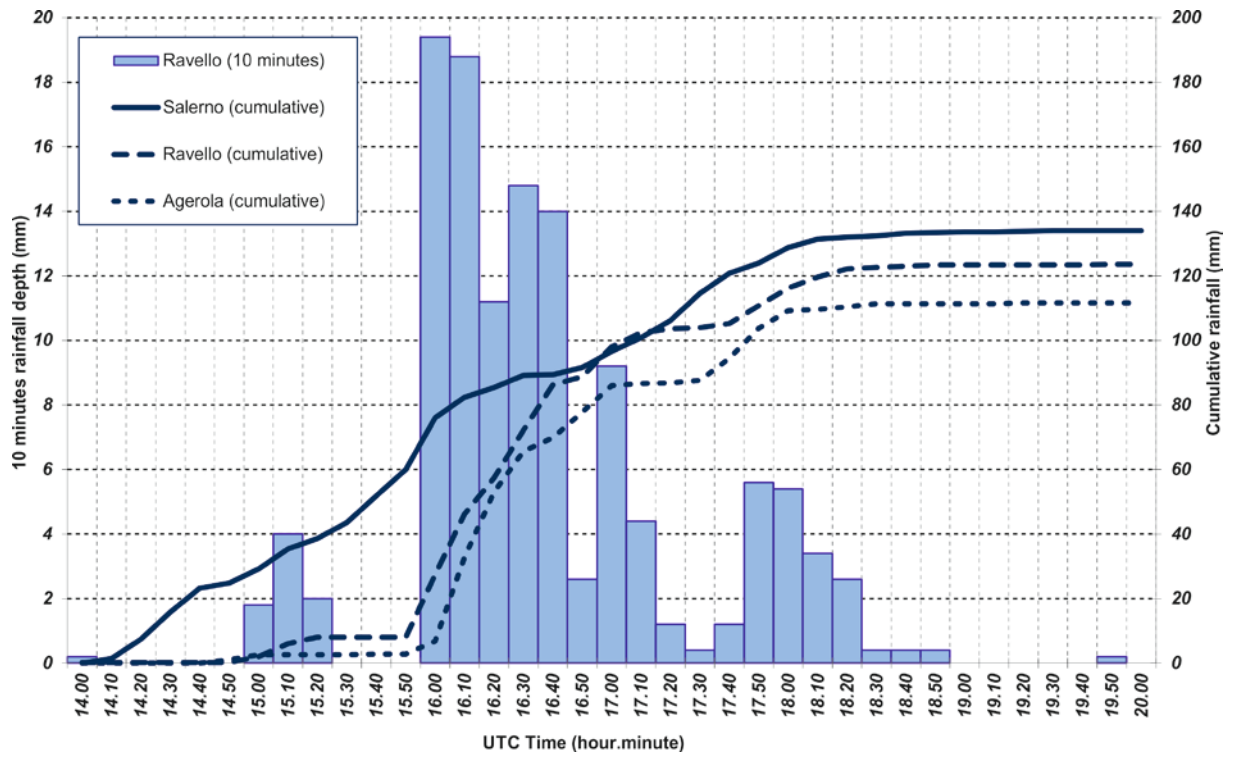
19

1 Figure 7



- 2
- 3
- 4
- 5
- 6
- 7
- 8
- 9
- 10
- 11
- 12
- 13
- 14
- 15
- 16
- 17

1 Figure 8



2

3

4

5

6

7

8

9

10

11

12

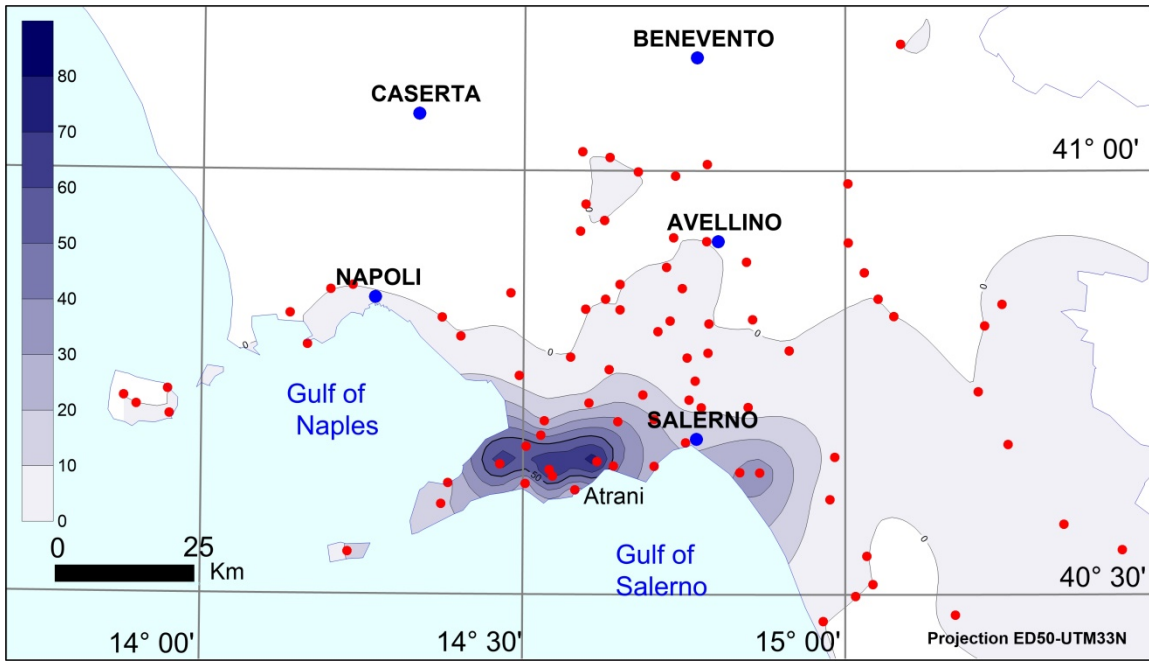
13

14

15

16

1 Figure 9



2

3

4

5

6

7

8

9

10

11

12

13

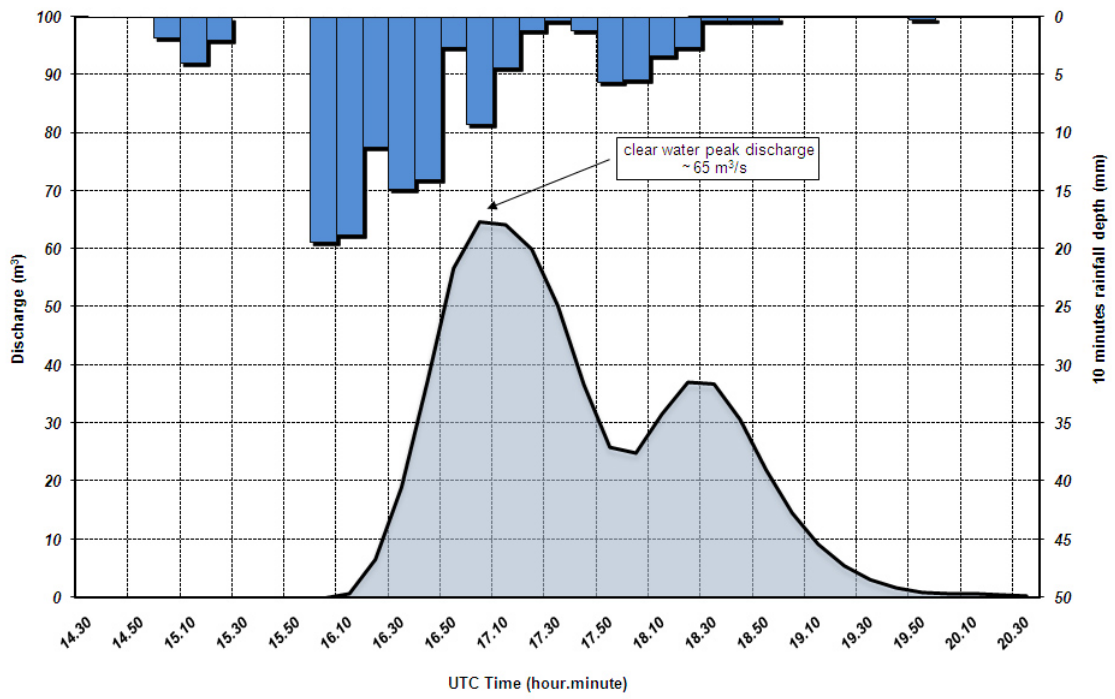
14

15

16

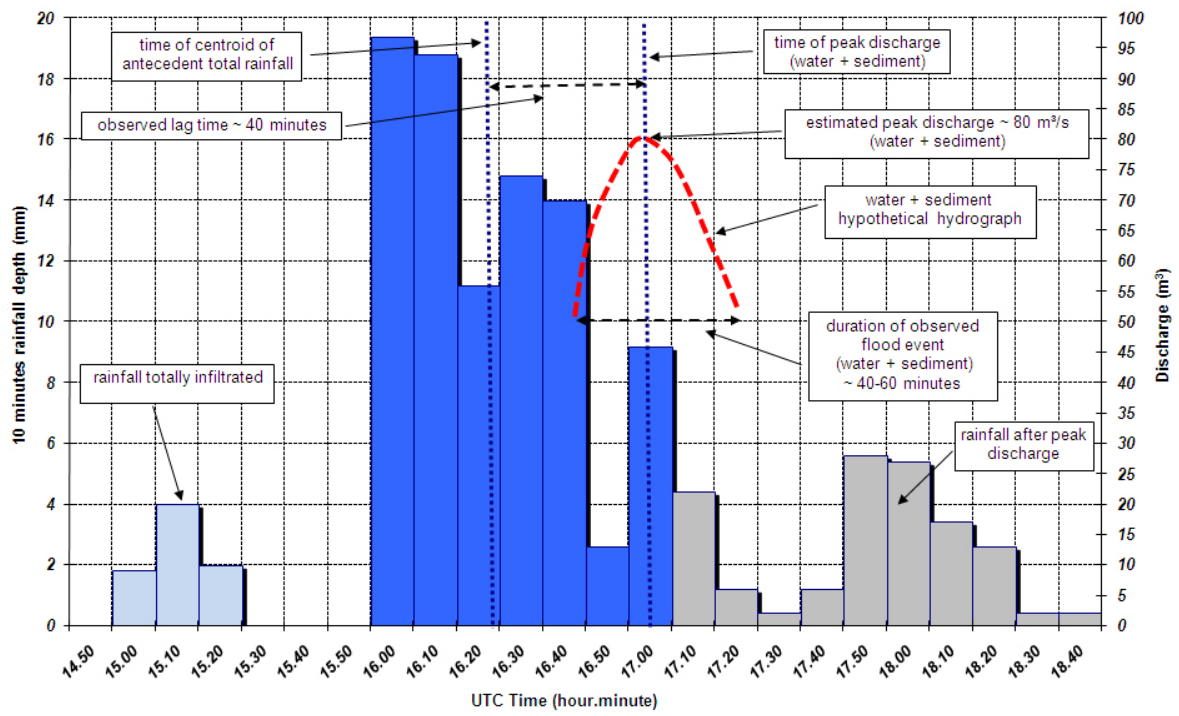
17

1 Figure 10



- 2
- 3
- 4
- 5
- 6
- 7
- 8
- 9
- 10
- 11
- 12
- 13
- 14
- 15
- 16

1 Figure 11



2

3

4

5

6

7

8

9

10

11

12

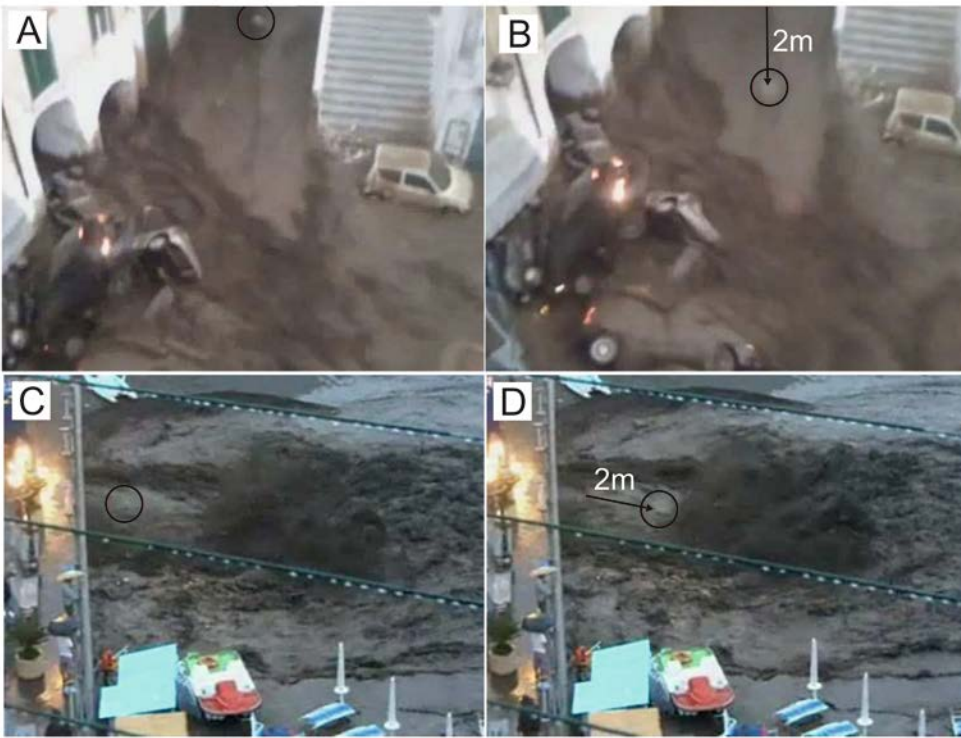
13

14

15

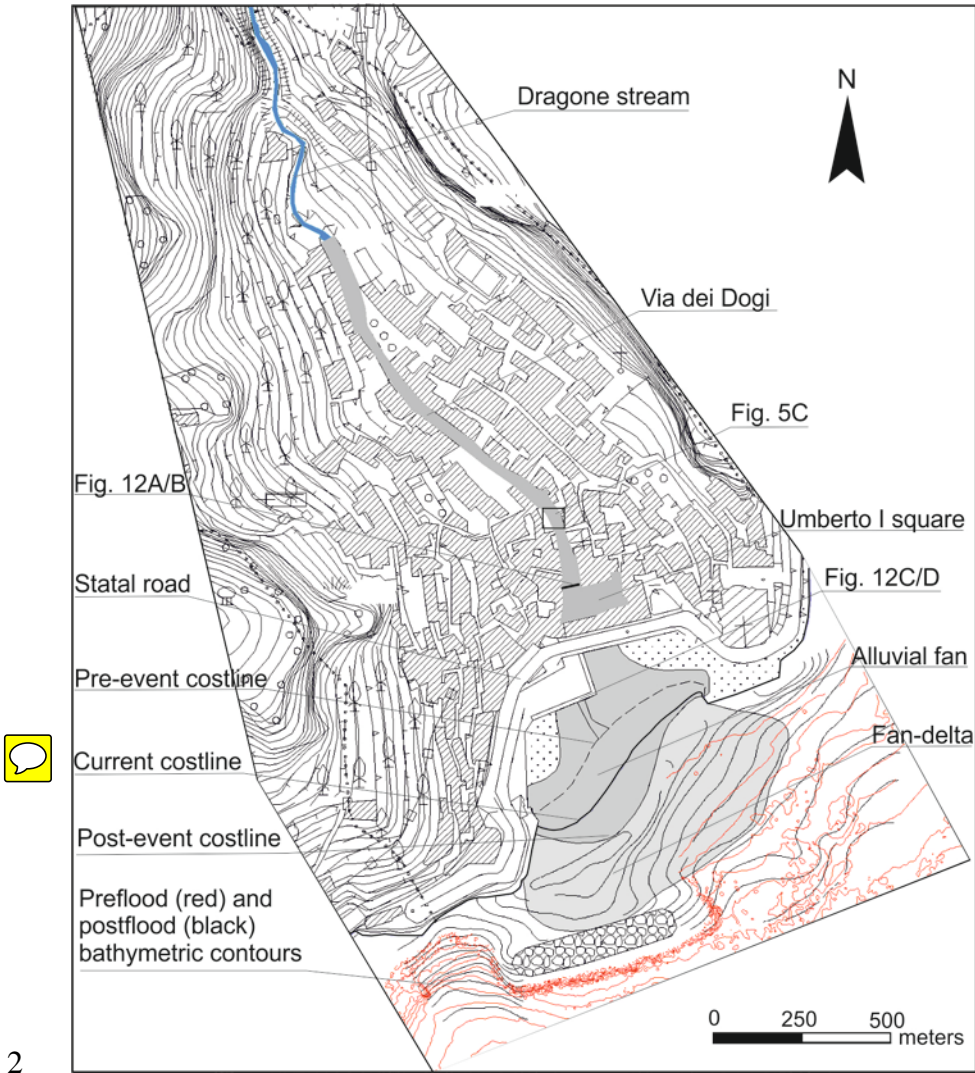
16

1 Figure 12



- 2
- 3
- 4
- 5
- 6
- 7
- 8
- 9
- 10
- 11
- 12
- 13
- 14
- 15
- 16

1 Figure 13



2

3

4

5

6

7

8

9

10

11

1 **FIGURE CAPTIONS**

2 Figure 1 - Geological sketch map and location of the study area (dashed box).

3 Figure 2 – The Amalfi rocky coast system characterized by steep and high watersheds,
4 urbanized alluvial-fan and fan-deltas at the mouth of main streams, reduced continental shelf
5 engraved by canyons, and abrupt shelf break (fault-controlled). The fan-deltas are composed
6 of prograding clinofolds resulting from flood activity as revealed by high-resolution seismic
7 profiles (inset map in the lower right corner). Modified from Violante, 2009 and Sacchi et al.,
8 2009.

9 Figure 3 - The Dragone catchment. (A) Basin elevation (DEM) and sub-basins of the Dragone
10 stream. 1. Scalandrone. 2. Nocelle. 3. Frezzi. 4. Senite. 5. S. Eustacchio. (B) slope map. Scale
11 for slope map is in the left lower corner.

12 Figure 4 - The Dragone-Canneto fan-delta body found off the Atrani village. Detail of a very
13 high-resolution seismic profile showing flood-controlled seismic-stratigraphic units and their
14 inferred association with major climatic changes of the last 2000 years. Letters A to L
15 represent age-dated stratigraphic horizons. See inset map for location (modified from Sacchi
16 et al., 2009).

17 Figure 5 – Geo-environmental effects induced by the September 9 2010 rainstorm in the
18 Dragone catchment. (A) Linear erosion engraving a tributary channel up to 2 m. (B) Soil slip
19 (arrows) at P. Castagne. (C) Partial outbreak of the main road (Via dei Dogi) in the Atrani
20 village. Red arrows indicate maximum height of the flow reaching ca 1 m above the street
21 pavement. Location in Fig. 13. (D) Site of temporary damming in correspondence of a man-
22 made structure built in the stream bed. (E) Terminal fan at mouth of the Dragone stream. See
23 Fig. 3 for location.

24 Figure 6 – (A) Visible-captured Meteosat-image on 09.09.2010 at 17:00 UTC (modified)
25 showing a mesoscale convective system (MCS) over the southern Tyrrhenian Sea and south
26 Italy. Inset: detail showing the Atrani storm cell. (B) Thunderstorm activity on 9 September
27 2010. Intense electric activity is recorded between 14:00 and 16:00 (sky-blue) near the city of
28 Salerno and between 16.00 and 18.00 (green) on the Amalfi Coast.

29 Figure 7 – (A) Rainfall intensity and air (min and max) and sea water temperatures measured
30 at Salerno from June 1 to September 30 2010; (B) Air and sea water temperatures at 10

1 minutes interval on September 9 2010. Data from Centre for weather forecast and monitoring
2 of the Campania Region (Biafiore et al., 2010).

3 Figure 8 – Cumulative rainfall at 10 minutes interval on September 9 2010 from 14:00 to
4 20:00 UTC as recorded by the rain gauges of Salerno, Ravello and Agerola. Rainfall intensity
5 at Ravello rain gauge is also reported. Data from Centre for weather forecast and monitoring
6 of the Campania Region (Biafiore et al., 2010).

7 Figure 9 – Isohyetal map of the cumulated rainfall from 16:00 to 16:50 UTC. Red dots are
8 rain gauges.

9 Figure 10 - Clear water hydrograph resulting from the hydrological model.

10 Figure 11 - Hyetograph and estimated flood peak discharge.

11 Figure 12 – Estimation of flow velocity from amateur videos by tracking selected particles
12 (black circle) transported by flood. (A) and (B) upper flow along via Dei Dogi. (C) and (D)
13 entombed flow at the Dragone stream mouth. Location in Fig. 13. See text for discussion.

14 Figure 13 – Map of the flooded area with indication of the alluvial-fan and the submerged
15 fan-delta.

16